

A Dissertation on
EFFECT OF PLASMA PARAMETERS ON THE GROWTH
AND FIELD EMISSION PROPERTY OF HEMISPHERICAL
CNT TIP

Submitted in the partial fulfillment of the requirements of the degree of
MASTER OF TECHNOLOGY

In

NUCLEAR SCIENCE & ENGINEERING (NSE)

By

ANIL KUMAR

2K14/NSE/05

Under the Guidance of

Prof. S. C. Sharma

(Supervisor)



Department of Applied Physics,
Delhi Technological University

(Formerly Delhi college of Engineering)

Govt. of NCT of Delhi

Main Bawana Road, Delhi-110042

JULY: 2016



Department of Applied Physics
Delhi Technological University (DTU)

(Formerly Delhi College of Engineering, DCE)

Govt. of NCT of Delhi

Bawana Road, Delhi-110042

CERTIFICATE

This is to certify that the Major project (AP-811) report entitled “**EFFECT OF PLASMA PARAMETERS ON THE GROWTH AND FIELD EMISSION PROPERTY OF HEMISPHERICAL CNT TIP**” is a bonafide work carried out by **Mr. Anil Kumar** bearing Roll No. **2K14/NSE/05**, a student of Delhi Technological University, in partial fulfilment of the requirements for the award of Degree in **Master of Technology** in “**Nuclear Science & Engineering**” (NSE).

As per the candidate declaration this work has not been submitted elsewhere for the award of any other degree/diploma.

(Prof. S. C. SHARMA)

Supervisor

Head, Department of Applied Physics,

Delhi Technological University,

Delhi-110042

DECLARATION

I declare that this written submission represents my ideas in my own words and where others' ideas or words have been included, I have adequately cited and referenced the original sources. I also declare that I have adhered to all principles of academic honesty and integrity and have not misrepresented or fabricated or falsified any idea/data/fact/source in my submission. I understand that any violation of the above will be cause for disciplinary action by the Institute and can also evoke penal action from the sources which have thus not been properly cited or from whom proper permission has not been taken when needed.

PLACE:

DATE:

ANIL KUMAR

(2K14/NSE/05)

ACKNOWLEDGEMENT

I take this opportunity as a privilege to thank all individuals without whose support and guidance I could not have completed my project successfully in this stipulated period of time.

First and foremost I would like to express my deepest gratitude to my supervisor **Prof. S.C. Sharma**, HOD, Applied Physics, for his invaluable support, guidance, motivation and encouragement throughout the period this work was carried out.

I am also thankful to **Mr. Ravi Gupta and Ms. Neha Gupta (Research scholars)** for their valuable support and guidance in carrying out this project.

I am deeply grateful to **Dr. Nitin K. Puri** (Assistant Professor, Applied Physics, Branch Coordinator, NSE) for his support and encouragement in carrying out this project.

I also wish to express my heartfelt thanks to staff at Department of Applied Physics of Delhi Technological University for their goodwill and support that helped me a lot in successful completion of this project.

Anil Kumar

ABSTRACT

This work presents a theoretical model to study the growth of carbon nanotube with hemispherical tip on the catalyst substrate surface in the presence of reactive plasma. The equation of charging of CNT, balance equation of ions, neutrals and electrons number density, growth equation of CNT and energy balance equation of CNT for hemispherical tip has been derived. The numerical calculation of growth of CNT has been carried out. From the result we get the effect of ion number density, substrate temperature, ion temperature and substrate potential on the height and radius of CNT. It is found that the height of CNT increases as ion density increases whereas radius of CNT decreases with increase in hydrogen ion density. Substrate temperature also has the effect on growth of CNT. The field emission properties have been analyzed from result obtained.

Contents	Page No
Chapter 1	1
1. Introduction	1
1.1 introduction to Carbon nanotube	1
1.2 structure of CNT	1
1.2.1 Single walled nanotube (SWCNTs)	1
1.2.2 Multi Walled carbon nanotube (MWCNTs)	2
1.3 Geometrical Structure and type of carbon nanotube	3
Chapter 2	
2. Growth of CNT and effect of Plasma on Growth of CNT	4
2.1 Growth of CNT	4
2.2 Arc discharge	5
2.3 Laser ablation	5
2.4 CVD	6
2.5 PECVD	7
2.5.1 Plasma	9
2.5.2 Working of PECVD	10
2.5.3 Ion bombardment	11
2.5.4 Catalyst Particle	12
Chapter 3	13
3. Theoretical model of Growth of CNT	13

3.1 Model	13
Chapter 4	21
4.1 Numerical Result and discussion	21
4.2 Matlab ODE solver used for solving the simultaneous equation	22
Chapter 5	27
5.1 Conclusion	27
References	28

List of figures	Page No
Fig. 1.1 Single Walled Carbon Nanotube	2
Fig. 1.2 Multi- Walled Carbon Nanotube	2
Fig.1.3 Structure of CNT	3
Fig. 2.1 Overview of synthesis method of CNT	5
Fig.2.2 Catalyst particle at the root of CNT Growth	6
Fig.2.3 Catalyst particle at the top of CNT Growth	6
Fig. 2.4 Schematic Diagram of PECVD	8
Fig. 2.5 Illustration and details regarding PECVD	9
Fig. 2.7 (a) Smaller particles are too active and dissolve too much carbon at the beginning. The excess carbon will form a thin layer of graphite that cover the surface of the catalyst particle and will cut the carbon supply to the particle, hence no SWCNT can grow. (b) Shows a moderate sized particle where SWCNT growth occurs. (c) The larger particles cannot efficiently catalyze the decomposition of carbon stocks which makes them unable to supply enough carbon to nucleate the SWCNT	12

List of Symbols

1. a:c : amorphous carbon
2. \sum : summation
3. \emptyset : electrostatic potential
4. γ_e : sticking co-efficient
5. γ_{CH_3} : sticking coefficient of CH_3
6. γ_{iA} : sticking coefficient of ion A
7. γ_{iB} : sticking coefficient of ion B
8. γ_A : thermal neutral atom sticking coefficient
9. T_e : electron temperature
10. T_i : ion temperature
11. T_s : substrate temperature
12. K_B : Boltzmann constant
13. h : height of CNT
14. r_{cnt} : radius of CNT
15. m_{cnt} : mass of CNT
16. n_e : electron number density
17. n_{iA} : ion number density of A type
18. n_{iB} : ion number density of B type
19. n_A : number density of neutral A
20. n_B : number density of neutral B
21. c_p : specific heat at constant pressure
22. m_c : mass of carbon
23. m_{iA} : mass of ion A
24. m_{iB} : mass of ion B
25. U_s : substrate potential
26. ρ : density of CNT
27. γ_0 : number of adsorption site per unit area
28. E_s : energy barrier for diffusion of carbon
29. D_s : surface diffusion coefficient
30. $\delta\epsilon_{th}$: activation energy of dehydrogenation
31. $\delta\epsilon_t$: energy due to thermal dissociation
32. P_i : partial pressure

CHAPTER 1

1. Introduction

1.1 Introduction to Carbon Nanotubes

Carbon nanotubes are the structural arrangement of carbon with a cylindrical nanostructure. These structures of carbon such as carbon nanotube, graphene, Bucky balls, graphite and diamond having only difference of hybridization of atoms of carbon. These carbon allotropes having typical properties which could be useful for the fields of nanotechnology, electronics, optics and some other fields like in materials. These carbon nanotubes are of sp^2 hybridization [1]. When graphene sheet is folded cylindrically we get single dimensional structure which is known as carbon nanotube. Due to their significant properties and specific function these carbon nanotubes are one of the most important structure of nanotechnology and Nano science. In the field of research carbon nanotube is very important due to their electrical and optical properties. Various work has been going in this field and other remarkable properties were discovered [2].

1.2 Structure of Carbon Nanotube

There is numerous way of process by which carbon nanotube structure is defined. One possibility is also that carbon nanotube is obtained by rolling a graphene sheet in a very specific direction, maintain the circumference of the cross section. Since the microscopic structure of the carbon nanotube is closely associated with graphene. Additionally, the reference to graphene will provide the theoretical deviation of many properties of carbon nanotubes. Fig. 1.1 and Fig. 1.2 shows the single walled and multiple walled carbon nanotube structure [3].

1.2.1 Single walled nanotubes (SWCNTs)

These types of carbon nanotubes are geometrically folding of graphene sheet to form a tube. Singled walled nanotubes diameter is in the range of few nanometers, but the tube length can be many millions of times of diameter. Singled walled carbon Nanotubes exhibit electrical properties that don't seem to be shared by the multi walled carbon Nanotubes variants. Especially their band gap will vary from 0 to 2 eV and their electrical property behavior is like

semiconductor and conductor in nature. Whereas the band gap of multi walled CNT is zero and it will only behave like a perfectly conductor [4].

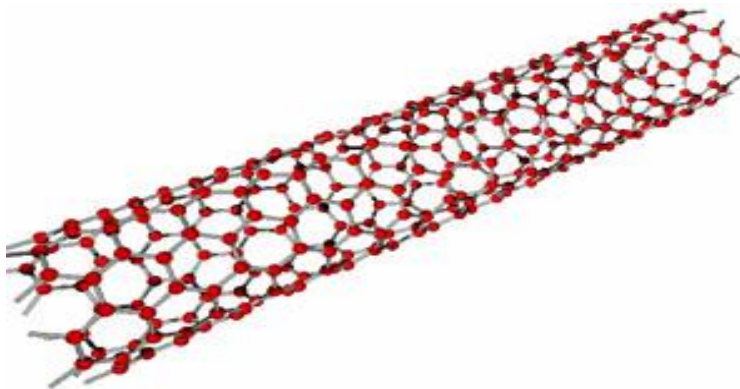


Fig. 1.1 Single Walled Carbon Nanotube

[<http://www.univie.ac.at/spectroscopy/fks/forschung/ergebnisse/nanotubes.htm>]

1.2.2 Multi Walled carbon nanotubes (MWCNTs)

Multi-walled carbon nanotube include many no of tubes in concentric cylinder, the number of concentric walls varies from 6 to 25 or more and the diameter of multi-walled carbon nanotube is in the range of 30 nm. These multi-walled carbon nanotube are highly conductive [5].

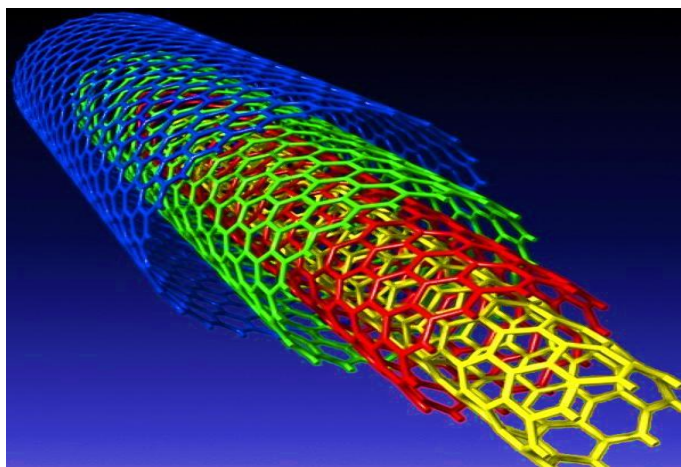


Fig. 1.2 Multi- Walled Carbon Nanotube

[<http://www.excel-metal.com/nanoparticles.html>]

1.3 Geometrical Structure and type of Carbon Nanotubes

single walled carbon nanotubes are represented by various ways such as rolling a graphene sheet and by rolling it posses certain plain of symmetry both parallel and perpendicular with the axis as shown in figure 1.3(a) & (c) while other do not show symmetrical property in 1.3 (b). when the folding in non symmetrical it is called as chiral or helical nanotube as they do not superimposed on their mirror image [6].

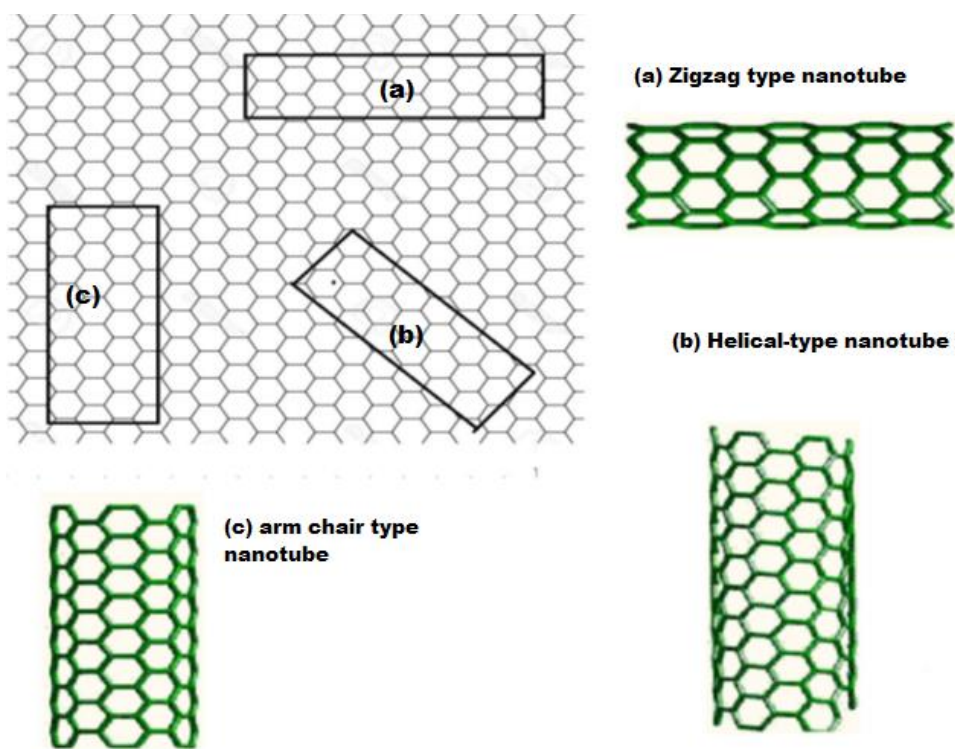


Fig.1.3 Structure of CNT

CHAPTER 2

2. Growth of CNT and Effect of Plasma on Growth of CNT

2.1 Growth of CNT

There are various methods used for fabrication of CNTs. The main aim is to find a technique that is easy, can produce cost effective CNTs of high quality, and with high rate of production and that produces CNTs with minimum defects. Additionally, it is more important to be able to control the diameter, chirality, the number of shells (for a MWCNT) and the purity, since all these parameters will influence the properties [7]. There are several methods for synthesis of CNTs, but three of them are considered as the general and widely known synthesis methods.

- I. Arc discharge
- II. Laser ablation
- III. Chemical vapor deposition

2.2 Arc discharge

This the first method used for the fabrication of CNT, It was originally used in the manufacturing of the C_{60} , due to its simplicity it one of the most common manufacturing methods. The mainly used arc discharge technique is the electric charge method, also called as the electric arc discharge. An electric arc discharge is produced between two graphite electrodes, which induces the graphite to vaporize and condense at the cathode. The process is done in the presence of inert atmosphere that consists of helium (He) or argon (Ar). Very high temperature is generated that allows transition of carbon from solid- to gas-phase without passing through an intermediate liquid phase [8]. The end product is soot that contains a complex mixture of fullerenes and other carbon structures, such as CNTs. To obtain them, purification by gasification with oxygen (O) or carbon dioxide (CO_2) is necessary since other carbonaceous material needs to be removed. The effect of gasification depends on the type of reactant that is used. To produce SWCNT there is need of a metal catalyst. The typical yield for this method is about 30% and it is capable of producing SWCNTs and MWCNTs [9].



Fig. 2.1 overview of synthesis method of CNT

[J. D. C. H. J. A. a. R. K. Jan Prasek, "Methods for carbon nanotubes synthesis—review," *Journal of Materials Chemistry*, vol. 21, p. 15872–15884, 2011]

2.3 Laser ablation

In this method it vaporizes a piece of graphite by treatment with a ND YAG laser in a chamber at 1200 °C in a flow of inert gas, such as He or Ar. The vapor is carried with the gas flow to a cooled wall of quartz tube where it condenses into a mixture of fullerenes and CNTs. The laser ablation method is capable of yield up to 70% and is able to produce SWCNTs and MWCNTs. It is particularly known to give SWCNTs of high quality and purity [10]. Nevertheless, the equipment requirements and the large amount of energy consumed in the synthesis by the arc discharge and the laser ablation method makes them less favorable in production of CNTs. Controlled synthesis on substrates with ordered CNT structures has not been possible for none of these two methods. The main technological drawback with these two methods is that neither one of them are able to produce CNTs directly on a surface, which means that they first need to be produced separately and then being manipulated onto substrates before use [11].

2.4 CVD

CVD is a parental to a clan of methods where deposition of a solid material on a surface is triggered by reactions with the predecessor gases in the chamber and the heated surface of the substrate. The growth process of the CNTs includes decomposition of carbon containing gases where carbon is diffused to a heated substrate which is coated with catalyst particles. The carbon impasses to Growth and properties of Carbon Nanotubes these and acts as a nucleation site for the origination of CNT growth. As long as the catalyst particles are supplied with carbon, the growth process continues and particle is either on top or at the bottom during CNT growth [12].

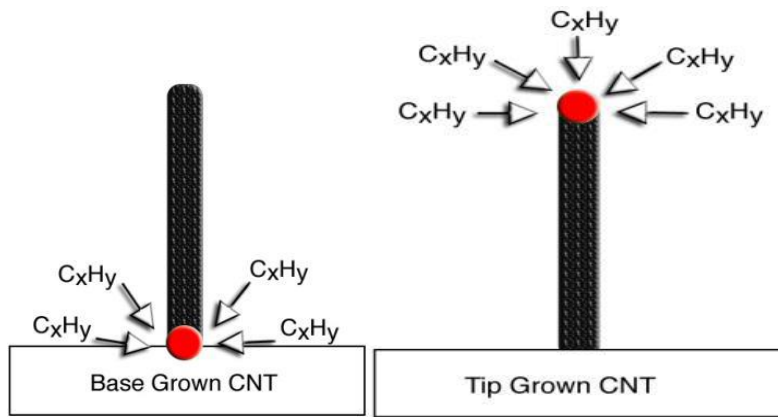


Fig. 2.2 catalyst particle at the Root of CNT Growth. Fig. 2.3 catalyst particle at the Top of CNT Growth.

[<http://www.aetherwavetheory.info/backup/chemie2/default.htm>]

The CVD process provides good control of the growth rate and the diameter. Type of CNT synthesized, depends on the temperature in the process and the size of the catalyst particle being used.

- I. Low temperature, 600-900 °C, favors the growth of MWCNTs
- II. High temperature, 900-1200 °C, favors the growth of SWCNTs

Since it is impossible to eradicate the catalyst particle during growth, post treatments are necessary. Such a treatment can be high temperature heat treatment or acid washing. During growth of CNT, it is common to find impurities, such as graphite compounds, amorphous carbon, fullerenes, coal and un-reacted metal particles. Since the target is CNTs of high purity, a purification step is required, which can be done by acid treatment, oxidative treatments in the gaseous phase/liquid phase and ultrasound methods [13].

The two most significant parameters in the synthesis of CNTs by CVD is the size of the catalyst particle and the carbon source. If the chosen carbon source is disapproving for growth conditions one can end up with a mixture of SWCNTs and MWCNTs, along with deposited amorphous carbon. The formed amorphous carbon during the CVD process coats the catalyst particle which reduces its activity and lifetime, and will affect the growth considerably [14].

The main benefit with CVD is that it permits more control over the morphology and structure of the formed CNTs and can give controlled alignment, such as producing small freestanding SWCNTs if the process parameters are controlled, instead of the “mixtures” which is obtained by the arc discharge and laser ablation method. In addition, CNTs can be produced directly on substrates without any further purification unless the catalyst particle is required to be removed.

The CVD is known to produce CNTs of high purity and offers a yield between 20 - 100%. Even though it possesses capable characteristics, the main problem with this method is the scalability and reproducibility in the production of CNTs [15].

2.5 Plasma Enhanced Chemical Vapor Deposition(PECVD)

PECVD and CVD use same gaseous sources, the most significant difference is that the CVD uses thermal energy to decompose the hydrocarbons, but in the PECVD the molecules are triggered by electron impact in the plasma. The disintegration takes place in non equilibrium plasma, which is often mentioned to as the glow discharge. The glow discharge is often generated by a high frequency power supply. As in the CVD, a catalytic particle is required to produce CNTs. The main purpose of using plasma is to reduce the activation energy which is needed for the deposition process. The growth temperature for producing CNTs in the PECVD could be lowered significantly; relative low substrate temperatures down to 300 °C can be used [16].

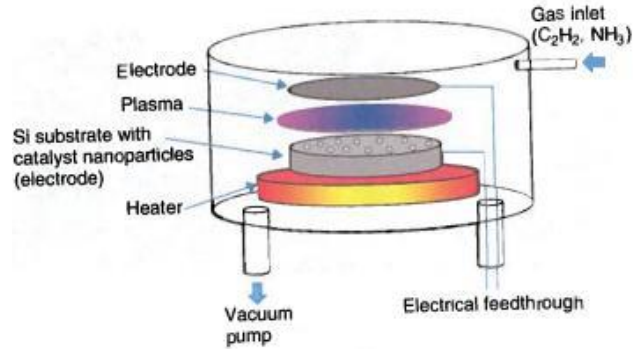


Fig. 2.4 Schematic Diagram of PECVD

[C. Binns, Introduction to Nanoscience and Nanotechnology, New Jersey: John Wiley & Sons, 2010, pp. 121-127.]

Due to the electric field which is produced by the high-frequency supply that is used to setup a time varying electric field between the plasma and the electrode, the CNTs are capable to grow perpendicular and allied on a surface, much like grass or pillars. This grants the option of creating pattern of catalysts, which means that it is possible to grow CNTs in selected regions on the sample's surface [17].

PECVD has become the method for the commercial growth of CNTs because of its simplicity, Controllability and the relative low synthesis temperature. Some of the drawbacks with the PECVD method today are that the preparation is quite cumbersome. For instance, the process of growing CNTs on stainless steel involves polishing, etching in hydrofluoric acid and hydrogen (H)/ammonia (NH₃) plasma pre-treatment to create the catalyst particles [18].

In addition, the evidence from most of Growth and properties of Carbon Nanotubes the CNT growth by PECVD up to now operates at almost equal temperatures as CVD which indicate the absence of the benefits by using plasma, and it is not really clear how the carbon diffusion step through the catalyst particle could be promoted by the plasma assistance yet Various works have been done to study the CNT growth of plasma, the subsequent effects of rf power density, temperature, rate of flow of gas on the growth rate, and dimensions of subsequent CNTs.

The core tasks of the plasma in CNT growth is of course to ionize the gas, as well as to cause a dissociation and diffusion of hydrocarbons into the catalyst particles and etch any a:C that may deposited on top of the catalyst particle thereby providing a Growth and properties of Carbon Nanotubes steady support of carbon atoms. The plasma is also likely to provide a heating effect to the sample, since it is subsequently exposed to conduction from hot gases as well as ion

bombardment. The additional heating effect leads to that less heat needs to be generated by the external heater [19].

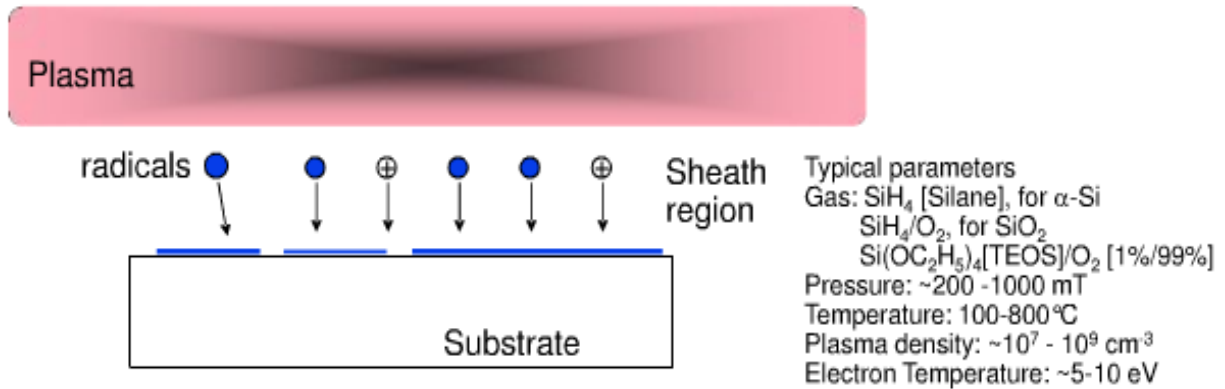


Fig. 2.5 Illustration and details regarding PECVD

[M. J. Goeckner, "Aspect of Plasma Processing: A brief overview of plasma science in industry," UTD, [Online]. Available:

http://www.utdallas.edu/~goeckner/plasma_sci_class/Plasma%20Process%203%20Types.pdf]

2.5.1 Plasma

Solid phase form when the thermal energy in a material is too low such that rigid bonds between the atoms can form. Liquid phase form when the thermal energy is too high to allow rigid bonds, but still low enough so that atoms stick to each other, just like slimy marbles. Gas phase form when the thermal energy is high enough, such that no atoms stick at all, then individual atoms is set free to fill the enclosure [20]. A further increase in temperature makes the molecules come apart into free ions and free electrons forming a fourth gaseous state of matter which is known as plasma. The new feature of this state which distinguishes it from an ordinary gas is that it conducts electricity. If there is enough energy to free weakly bound electrons, there is also enough to promote more deeply bound electrons to excited states which is why almost all plasmas glows in the dark, such as stars, fluorescent lights, flames, the northern and southern lights, meteor trails [21].

2.5.2 Working of PECVD

To be able to understand the mechanism that is involved in the growth of CNTs, the basic processes that occur in the plasma must be understood. The direct current (DC) reactor is the simplest case, where a DC voltage is applied across a space filled with low pressure gas. The glow discharge that is initiated can be divided into three regions that are visible, and is arranged from cathode to anode [22].

- I. cathode dark space
- II. negative glow
- III. faraday dark space

The DC discharge is maintained by the processes at the cathode and in the dark space which creates an electrical field. Due to this field, growth of vertically aligned carbon Nanotubes (VACNTs) is possible as it forces the CNTs to align in the direction of the field as they grow. The ions are accelerated by the applied voltage and some of them bombard the cathode which causes generation of secondary electrons that are accelerated away from the cathode. The collisions excite molecules, and energetic electrons ionize some of them, which is the reason for the negative glow. The thickness of the dark space is related to the electron mean free path. The current in it is primarily carried by ions, while the current in the negative glow is primarily carried by electrons. Thus, the negative glow has a low impedance region and most of the applied voltage drops over the dark space. Since it varies from a few hundred μm to a few mm , several hundred volts can be created in the electric field, such as in the order of 10^3 V/mm [23].

The radicals that are produced in the plasma and the supplied feed gas drifts to the substrate Surface. The radicals does not chemically react with the substrate, instead they combine to form Stable chemicals (solids). Ions are accelerated across the sheath which delivers energy that is driving the chemical reaction(s) between the radicals and the surface material. Since hydrocarbon decomposition is better activated by molecule collisions (plasma) and is done at a much faster rate than by thermal pyrolysis, lower processing temperature should be allowed which makes the PECVD more beneficial than pure CVD methods. The activation energy for the breakdown of reactive species and their subsequent interaction with other species to form a deposit in the PECVD is provided by the high kinetic energy of electrons in the plasma [24].

The electron density in the radio frequency PECVD (RF-PECVD) is much higher than in the direct current PECVD (DC-PECVD) since DC waste a lot of its input power on accelerating the ions whereas the desire is to use the power efficiently for generation of reactive species. Higher electron densities result in higher ionization rates since the electrons are responsible for the ionization rate and for the formation of reactive free radicals. One major advantage with the RF is therefore its efficient decomposition of gas molecules and a clear difference is the higher number of H ions present in RF, that can enhance the activity of the metal catalysts by reduction and increase in the wetting ability. In addition, RF can also facilitate etching of a:C [25].

It is the best suited plasma source for deposition on large areas as the plasma is very stable and homogenous. Because of the higher density of reactive radicals and the stability, the RF-PECVD seems to be preferred for growing CNTs at low temperatures. The trend in the industry is to move away from DC reactors and towards higher frequency plasma reactors. The effect of 180 °C in the PECVD appears to be comparable to that of 750 °C in the CVD [26].

The main tasks of the plasma in CNT growth is of course to ionize the gas, as well as to cause a dissociation and diffusion of hydrocarbons into the catalyst particles (which also depends on the Temperature) and etch any a:C that may deposited on top of the catalyst particle thereby providing a steady support of carbon atoms. The plasma is also likely to provide a heating effect to the sample, since it is subsequently exposed to conduction from hot gases as well as ion bombardment. The additional heating effect leads to that less heat needs to be generated by the external heater.

2.5.3 Ion bombardment

There is uncertainty whether bombardment is favorable or not for growth of CNTs. Some believes that bombardment during CNT growth can introduce lattice defects which cause bending and alternations of its diameter. How serious these defects are depends on the synthesis temperature. When temperatures above 600 °C have been used, no damage by ion bombardment to the CNTs has Growth and properties of Carbon Nanotubes been recorded, but when lowered below 500 °C the growth rate is significantly decreased, which is most likely because that the ion etching rate exceeds the growth rate [27]

2.5.4 Catalyst Particles

Since the quality and the structure of CNTs depends greatly on the properties and the type of catalyst material being used, it is essential to study the catalysts. A key factor for controlling the diameter and the number of shells in a CNT is to gain control of the catalyst particle's diameter, since they are the basis of the grown CNTs. This means that growing SWCNTs requires a strict diameter control, and what usually makes it easier to produce MWCNTs. The generally considered proper sized of Nano-particles to initiate SWCNT growth is approximately 1 nm.

One of the challenging tasks with catalyst particles is that it is difficult to define a specific relation between the size of them and the resulting diameter of the CNT. Such factors have to do with the reduced size and subsequent exhaustion of catalyst material during growth. This is believed to be because of to ion-beam sputtering, loss of catalyst material due to evaporation of metal atoms at high temperatures and dissolution of carbon species which tends to change the size of the particles during synthesizing. One of the major functions of the catalyst particle during growth is to function as an etch mask, by protecting the core of the growing nanostructure from physical and chemical etching [28]. Only moderate size particles ensures a suitable carbon supply for nucleation and growth of SWCNTs at a given carbon feed rate which is given in fig. 2.7.

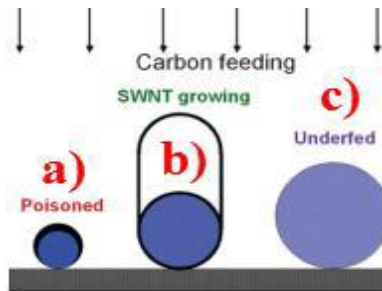


Fig. 2.7 (a) Smaller particles are too active and dissolve too much carbon at the beginning. The excess carbon will form a thin layer of graphite that cover the surface of the catalyst particle and will cut the carbon supply to the particle, hence no SWCNT can grow. (b) Shows a moderate sized particle where SWCNT growth occurs. (c) The larger particles cannot efficiently catalyze the decomposition of carbon stocks which makes them unable to supply enough carbon to nucleate the SWCN

[S. a. J. R. C.T. Wirth, "State of catalyst during carbon nanotube growth," *Diamond & Related Materials*, vol. 18, pp. 940-945, 2009]

CHAPTER 3

Theoretical Model of Growth of CNT

3.1 Model

In this model, we study the evolution of the CNT with hemispherical tip on the catalyst–substrate surface in the presence of reactive plasma containing electrons, positively charged ions of methyl (CH_3^+) represented as ions A and hydrogen ions (H^+) represented as ions B, neutral atoms of type A methane (CH_4), and neutral atoms of type B hydrogen (H_2). We are taking Silicon (Si) as substrate and Nickel (Ni) as the catalyst. The reactive plasma of Ar^+ , H_2^+ , CH_4 is taken and CH_4 acts as a main source of carbon. As catalyst-substrate surface is in contact with the plasma, In this model, we consider sheath kinetics. The direction of electric field produced due to the separation of charge within the sheath region is along the z-axis [29].

The continuity equation [30].

$$\frac{\delta n}{\delta t} + \nabla \cdot (nu) = K - N$$

K and N are the left over terms due to the collision part of the Boltzmann equation

$$K = V_{ij} n_e$$

continuity equation modifies to

$$\nabla \cdot (nu) = V_{ij} n_e, \quad (3.1)$$

where n_e is electron number density, V_{ij} is ionization frequency, n and u shows the number density and fluid velocity of electrons, by taking the effect of CH_3^+ , CH_2 , Ar^+ and H^+ ion momentum balance equation

$$M n_j u_j \frac{du_j}{dz} = e n_j E - M n_j V_{jn} u_j. \quad (3.2)$$

Here M is the mass of ions in plasma, u_j is the fluid velocity, n_j is no density, V_{jn} is the collision frequency and E is the electric field.

To find out the potential within the sheath we use Poisson's equation

$$\frac{d^2\phi}{dz^2} = -4\pi \sum q_j \delta_j n_j \quad (3.3)$$

ϕ is the electrostatic potential, δ_j is the j^{th} ion to electron density.

I. Charging of CNT

This equation shows how the charge is developed on the CNT (i.e., a hemispherical tip over the cylindrical surface) due to diffusion of positively charged ions and accumulation of electrons on the surface of CNT (hemispherical tip over the cylindrical surface). Following Tewari and Sharma [31], we can write

$$\frac{dQ}{dt} = I_{iAc} + I_{iAcs} + I_{iBc} + I_{iBcs} - \gamma_e (I_{ec} + I_{ect}). \quad (3.4)$$

Here Q is the charge over the CNT (i.e., a hemispherical tip over the cylindrical surface)

where

$$I_{ec} = A \sqrt{\frac{8K_B T_e}{m_e}} n_e(x) \exp\left(Q\alpha_e + \frac{eV_s}{K_B T_s}\right)$$

It is the electron collection current at the surface of hemispherical tip, $A = \frac{\pi r_{cnt}^2}{2}$ is the area of the hemispherical tip.

$n_e(x) = n_{e0} \exp\left(\frac{e|\phi(x)|}{K_B T_s}\right)$ is electron number density in plasma sheath, $\phi(x)$ is electrostatic potential

$$\phi(x) = \phi_0 \exp\left(-\frac{|x|}{\lambda_d}\right)$$

and $\alpha_e = \frac{e^2}{r_{cnt} K_B T_e}$, ϕ_0 is the negative potential at the surface and λ_d is the debye length.

$$\lambda_d = \sqrt{\frac{K_B T_e}{n_e e^2}}$$

$$I_{ect} = n_e(x)r_{cnt}h\left(\frac{2\pi K_B T_e}{m_e}\right)\exp\left(\frac{eV_s}{K_B T_e} + \frac{eU_s}{K_B T_e}\right)$$

I_{ect} is electron collection current on the CNT cylindrical surface and V_s surface potential on the cylindrical surface of the CNT and h is the height of the cylindrical surface of CNT, m_e is the mass of electron [32].

$$I_{ijcs} = n_{ij}(x)r_{cnt}h\left(\frac{2\pi K_B T_i}{m_{ij}}\right)\left\{\frac{2}{\sqrt{\pi}}\sqrt{\frac{eV_s}{K_B T_i}} + \exp\left(\frac{eV_s}{K_B T_i}\right)\operatorname{erfc}\left(\sqrt{\frac{eV_s}{K_B T_i}}\right)\right\}\exp\left(-\frac{E_b}{K_B T_s}\right)\exp\left(-\frac{eU_s}{K_B T_s}\right)$$

It is the ion collection current on the cylindrical surface of CNT, T_i is the ion temperature, m_{ij} is the ion mass where j refers type of charge i.e. , type A or type B.

$$I_{ijc} = A\left(\sqrt{\frac{8K_B T_i}{\pi m_{ij}}}\right)n_{ij}(x)(1 - Q\alpha_i)\exp\left(-\frac{E_b}{K_B T_s}\right)\exp\left(-\frac{eU_s}{K_B T_s}\right)$$

It is the ion collection current to hemispherical tip of CNT, $A = \frac{\pi r_{cnt}^2}{2}$ is the area of the hemispherical tip.

where $n_{ij}(x) = n_{ijo}\left(1 - \frac{2e\phi(x)}{m_i v_{i0}^2}\right)$ shows ion density in plasma sheath, v_{i0} is ion velocity at any point within the plasma and $\alpha_i = \frac{e^2}{r_{cnt} K_B T_i}$

when substrate bias potential increased CNT develops more negative charge on the surface this would increase the thickness of plasma sheath and this increase the negative substrate bias and it accelerates the positive ion species [32].

II. Growth rate equation of electron density

The equation shows the balance of electron number density in the plasma bulk on process of ionization, recombination, and electron collection current coefficient of ionization of the constituent neutral atoms due to external field is given by β_j . Following Tewari and Sharma [31], we can write

$$\frac{dn_e}{dt} = (\beta_A n_A + \beta_B n_B) - (\alpha_A n_e n_{iA} + \alpha_B n_e n_{iB}) - \gamma_e n_{ct} (I_{ec} + I_{ect}). \quad (3.5)$$

$\alpha_j(T_e) = \alpha_{j0} \left(\frac{300}{T_e}\right)^k$ is coefficient of recombination of positively charged ions and electrons.

n_e is an electron number density n_{iA} and n_{iB} are the ion no density of ions A and B respectively.

In the Eq. (3.5) first term shows the rate of gain in electron density per unit time due to ionization of neutral atoms; the second term is the decaying rate of the electron density due to electron-ion recombination. The last term is electron collection current at the surface of the CNT (Hemispherical tip over the cylindrical surface) [33].

III. Growth rate equation of positively charged ion density

The equation shows the balance of positively charged ions in plasma bulk due to ionization of neutral atoms, recombination of ions and electrons, ion collection current at CNT surface, their adsorption, desorption, and thermal dehydrogenation. Following Tewari and Sharma [31], we can write

$$\frac{dn_{iA}}{dt} = (\beta_A n_A - \alpha_A n_e n_{iA}) - n_{cnt} (I_{iAc} + I_{iAcs}) - \varphi_{aiA} + \varphi_{desorption} \quad (3.6)$$

$$\frac{dn_{iB}}{dt} = (\beta_B n_B - \alpha_B n_e n_{iB}) - n_{cnt} (I_{iBc} + I_{iBcs}) - \varphi_{aiB} + \varphi_{desorption} + \varphi_{th} \quad (3.7)$$

where adsorption flux on top of the catalyst substrate surface is $\varphi_{aij} = \frac{P_i \gamma}{\sqrt{2\pi m_{ij} k_B T_i}}$, P_i is the partial

pressure of adsorbing species, $\varphi_{desorption} = \varphi_{ij} \gamma \exp\left(-\frac{\varepsilon_{ai}}{k_B T_{ij}}\right)$ is the desorption flux from the

catalyst-substrate surface, j refers to type of ions A or B, γ is the thermal vibrational frequency,

E_{ai} is the adsorption energy, φ_{ij} is the ion flux on the catalyst substrate surface [34].

$\varphi_{th} = \varphi_H \gamma \exp(-\frac{\delta \varepsilon_{th}}{K_B T_s})$ is the flux of type B ion (H^+) on report of thermal dehydrogenation. $\delta \varepsilon_{th}$ is the activation energy of thermal dehydrogenation, φ_H is the hydrogen ion flux at catalyst-substrate surface. The first term in Eqs. (3.6) and (3.7) shows about the gain in ion density per unit time on the basis of ionization of neutral atoms, the second term is electron-ion recombination. The third term is ion collection current to the surface of the CNT (hemispherical tip over the cylindrical surface). The fourth term is loss of ions on account of their adsorption to the catalyst-substrate surface and fifth term is the gain of ion density due to the desorption ion of ions from the catalyst-substrate surface into plasma. The last term in Eq. (3.7) explains the increase of hydrogen ion number density in plasma due to thermal dehydrogenation [35].

IV. Growth rate equation of neutral atom

The equation shows the balance of neutral particles in plasma due to recombination of electrons-ions, ionization of neutral molecules, ion and neutral collection current on the CNT surface. Following Tewari and Sharma [31], we can write

$$\frac{dn_A}{dt} = (\alpha_A n_e n_{iA} - \beta_A n_A) + n_{cnt}(1 - \gamma_{iA})(I_{iAc} + I_{iAcs}) - n_{cnt}\gamma_A(I_{Ac} + I_{Acs}) \quad (3.8)$$

$$\frac{dn_B}{dt} = (\alpha_B n_e n_{iB} - \beta_B n_B) + n_{cnt}(1 - \gamma_{iB})(I_{iBc} + I_{iBcs}) - n_{cnt}\gamma_B(I_{Bc} + I_{Bcs}) \quad (3.9)$$

where neutral collection current at the surface of Hemispherical tip of CNT is I_{jc} and

$$I_{jc} = A \sqrt{\frac{8K_B T_n}{\pi m_j}} n_j, A = \frac{\pi r_{cnt}^2}{2}$$

is the area of hemispherical tip, $I_{jcs} = \pi r_{cnt} h \sqrt{\frac{2K_B T_n}{m_j}} n_j$ is the collection current on the cylindrical surface of CNT.

γ_{iA} is the ion sticking coefficient and γ_A is the neutral atom sticking coefficient, T_n is the neutral atom temperature, n_j is the neutral atom density, and m_j is the neutral atom mass. The first term in Eqs. (3.8) and (3.9) is gain in neutral atom density per unit time due to electron-ion recombination; the second term is the decrease in neutral density due to ionization. The third term is the gain in neutral density due to neutralization of the particles collected at the open of the CNT. The last term is the accumulation of neutral atoms of species A and B on the surface of the CNT [36].

V. Growth rate equation of the curved surface area of CNT

Following Tewari and Sharma [31], we can write

$$r_{cnt} \frac{d(2\pi h)}{dt} = \left[\{ 2n_{cH}\gamma \exp\left(-\frac{\delta E_t}{K_B T_s}\right) + 2\theta_{cH}\varphi_{iA}\gamma_d + 2\varphi_{iA} + \varphi_{iA}\sigma_{ads}\varphi_{iB} + \varphi_c \} m_c + \right. \\ \left. \{ \varphi_{iA}(1 - \theta_t) + \varphi_{iA}\sigma_{ads}\varphi_H + \varphi_{iA}\gamma \exp(-\delta E_t/K_B T_s) \} m_{iA} \right] \frac{D_s 2\pi r_{cnt}}{\pi r_{cnt}^2} I_{iAcs} + \gamma_{CH3cs} \quad (3.10)$$

$$\frac{d(2\pi r_{cnt}^2)}{dt} = \left\{ \varphi_{iB}\gamma \exp\left(\frac{E_b}{K_B T_s}\right) + \varphi_{iB}\gamma \exp\left(\frac{-\delta E_{th}}{K_B T_s}\right) + \varphi_{iB}(1 - \theta_t) + \varphi_{iB} + \theta_{cH}(\varphi_{iB}\gamma_d + \right. \\ \left. \gamma_0 \gamma \exp\left(\frac{\delta E_i}{K_B T_s}\right)) \right\} \frac{h(t)}{n_{iB}} \quad (3.11)$$

VI. Energy balance of Hemispherical CNT Tip.

$$\frac{d}{dt}(m_{cnt} C_p T_{cnt}) = n_{ect} \left[\gamma_e \varepsilon_{ec}^s + (1 - \gamma_e) \gamma_{ect} \left(\varepsilon_{ect}^s - \frac{3}{2} K_B \right) T_{cnt} \right] - \frac{3}{2} K_B [n_{Act} \{ \gamma_A T_n + \\ \delta_{Act}(1 - \gamma_A) \} (T_n - T_{cnt}) + n_{Bct} \delta_{Bct} (T_n - T_{cnt})] + [n_{iAct} (\varepsilon_{iAs}^s + I_{pA}) + n_{Bct} (\varepsilon_{iBs}^s + I_{pB})] - \\ \frac{3}{2} K_B [(1 - \gamma_{Ai}) n_{iAct} + n_{iBct}] T_{cnt} - 4\pi a^2 \left\{ \varepsilon \sigma (T_{cnt}^4 - T_a^4) + \left[n_A \sqrt{\frac{8K_B T_n}{\pi m_A}} + n_B \sqrt{\frac{8K_B T_n}{\pi m_B}} \right] K_B (T_{cnt} - \right. \\ \left. T_n) \right\}. \quad (3.12)$$

Where m_{cnt} is the mass of the carbon nanotube, $m_{cnt} = (V_{hemispherical\ tip} +$

$V_{cylindrical\ surface})\rho$, after expanding both the term we get $m_{cnt} = (\frac{2}{3}\pi r_{cnt}^3 + \pi r_{cnt}^2 h)\rho$.

$\varepsilon_{ijc}^s(Z) = \left[\left(\frac{2-Z\alpha_{ji}}{1-Z\alpha_{ji}} \right) - Z\alpha_{ji} \right] K_B T_i$ shows the mean energy collected by ions at the surface of CNT.

This equation is divided in five parts, the first three term shows about the rate of energy transferred to CNT surface due to sticking accretion and elastic collision by constituent species of plasma. The last carried away by the neutral species (generated by the recombination of the accreted ions and electrons) from the CNT per unit volume per unit time. The last term is the rate of energy dissipation through radiation and conduction from the gas present.

where $n_{cH} = \theta_{cH}\gamma_0$ is the number density, θ_{cH} is the total surface coverage of either C_2H_2 or CH_4 in this case, $\varphi_c = n_{cH} \frac{v_{thc}}{4}$ of the ion flux carbon ions and v_{thc} is the thermal velocity of C

ions, δE_t is the thermal barrier, $\varphi_{iA} = n_{iA} \frac{K_B T_i}{m_{iA}}$ and $\varphi_{iB} = n_{iB} \frac{K_B T_i}{m_{iB}}$ are the ion flux of type A and type B.

Equations (3.10) and (3.11) reflects how the development of the CNT on catalyst nanoparticle takes place. The Eq. (3.11) deals with the height of CNT. The value of the height of the cylindrical part of the CNT at time t is then served into Eq. (3.11) to determine the CNT radius CNT (r_{cnt}). Equation (3.11) precisely calculates the curved surface of the spherical CNT tip. In Eq. (3.10), the first term in the first bracket defines the production of carbon atoms on the catalyst surface due to thermal dissociation of methyl ions (with energy barrier δE_t), second term defines the ion induced dissociation of CH_4 . The third term signifies the decomposition of positively charged ions of type A. The fourth term is the interface of ions with atomic hydrogen from the plasma, fifth term is explanations for the incoming flux of carbon atoms per unit time onto the catalyst particle. Similarly, the sixth term signifies the adsorption of type A ions to the surface, seventh term is the interaction of adsorbed type A ions with atomic hydrogen from plasma, and the eighth term is due to thermal dissociation of carbon source gas.

The I_{iAcs} is explanations for the ion collection current on the growing cylindrical part of the CNT. The term $\frac{D_s 2\pi r_{cnt}}{\pi r_{cnt}^2 \rho_p}$ denotes the surface diffusion of species onto the catalyst surface across the catalyst nanoparticle per unit area mass density. Finally, the last term denotes the sticking of neutral atoms of methane to the cylindrical surface of the CNT.

In Eq. (3.11), the first term signifies hydrogen atom diffusing into the catalyst-substrate surface, the Second term is explanation for the incoming flux of hydrogen ion due to thermal dehydrogenation of type A ions, third term is adsorption of type B ions to the surface. The fourth term is the decomposition of positively charged ions of type B, fifth term is due to ion induced dissociation of CH_4 , sixth term is due to the incorporation of hydrogen ions due to thermal dissociation of methyl ions. Equation (3.11) explains only for the nanoparticle tip radius as bottom area is already determined by the catalyst nanoparticle because they are source of nanoparticle growth $h(t)$ is the height of CNT with time t .

CHAPTER 4

4.1 Numerical Result and Discussion

This work shows theoretical model of CNT growth on the presence of catalyst surface in reactive plasma. Reactive plasma comprises of numerous reactive species that frequently transform into each other and new species as a consequence of numerical chemical reaction in ionized form. Meanwhile throughout the nanostructure synthesis there are several processes involved like dissociation, ionization, recombination etc., due to this, we consider reactive plasma in our present model in its place of the multi component plasma.

In this model we assume that, the applied plasma power produces active species plasma, which dissociates the catalyst particle into Nano-clusters required for CNTs nucleation and growth. In a plasma medium, following processes takes place, specifically ionization (in which a neutral atom gives rise to an ion) and recombination (of an ion with an electron results in a neutral molecule), adsorption (absorption on the surface), desorption of ionic species, thermal dehydrogenation (removal of hydrogen), evaporation and their diffusion (surface) into catalyst surface and sticking of neutral atoms to the CNT surface. Since, the substrate-catalyst surface is in contact with the plasma, the inevitable plasma sheath is molded close to the surface in contact with the plasma. Due to plasma sheath, the electric field is directed from plasma bulk towards the surface that accelerates the ions towards the surface, and then the effect of electron and ion collection current to the CNT surface due to plasma sheath has been consider in the present model. The CNT considered in the present paper is SWCNT.

4.2 The Matlab ODE solvers used to solve simultaneous equation

$$\frac{dx_1}{dt} = f_1(x_1, x_2, x_3, \dots, t)$$

$$\frac{dx_2}{dt} = f_2(x_1, x_2, x_3, \dots, t)$$

$$\frac{dx_3}{dt} = f_3(x_1, x_2, x_3, \dots, t)$$

.....

The Matlab ODE solvers are accessed by calling a function of the form

[X, T]=ode solver name (@function name, time span, x_0); where @function name=It handle to a function which returns a vector of rates of change time span = a row vector of times at which the solution is needed OR a vector of the form[start, end].

x_0 = a vector of initial values

solver	Implicit/explicit	Accuracy
Ode45	Explicit	4 th order, medium accuracy
Ode23	Explicit	2 nd /3 rd order, low accuracy
Ode113	Explicit	Very accurate (13 th Order)
Ode15s	Implicit	Anything from 1 st -5 th order
Ode23s	Implicit	Low accuracy (but may be more stable than ODE15s)
Ode23tb	Implicit	Low accuracy (but may be more stable than ODE15s)

We have simultaneous solve equation (3.4)-(3.11) which has been developed in theoretical model, here for the solution of these differential equation we are using ode15s.

ODE15s should only be used for stiff problems. Because it is an implicit scheme, it will have to solve (possibly large) sets of equations at each time step.

At each time step, ODE15s will solve a set of linear or non-linear equations, for which it will require the Jacobian of F(t, x) . Since the routine was given no information on the Jacobian, it is forced to calculate the full Jacobian, numerically.

After solving these ordinary differential equation we get the dependence of the height and radius of the CNT on the plasma parameter (i.e., ion density of both type A and B ions and temperature and pressure) by simultaneous solution of Eqs.(3.1)–(3.11) at appropriate boundary conditions.

At t=0, Q = -1 C, electron no density $n_{e0} = 1.12 \times 10^{10}$, ion number density $n_{iA0} = 6.72 \times 10^9$, $n_{iB0} = 4.48 \times 10^9$, neutral atom density $n_{A0} = 10^{15}$, $n_{B0} = 10^{15}$, initial height h=50 nm, initial radius $r_{cnt} = 50 \text{ nm}$.

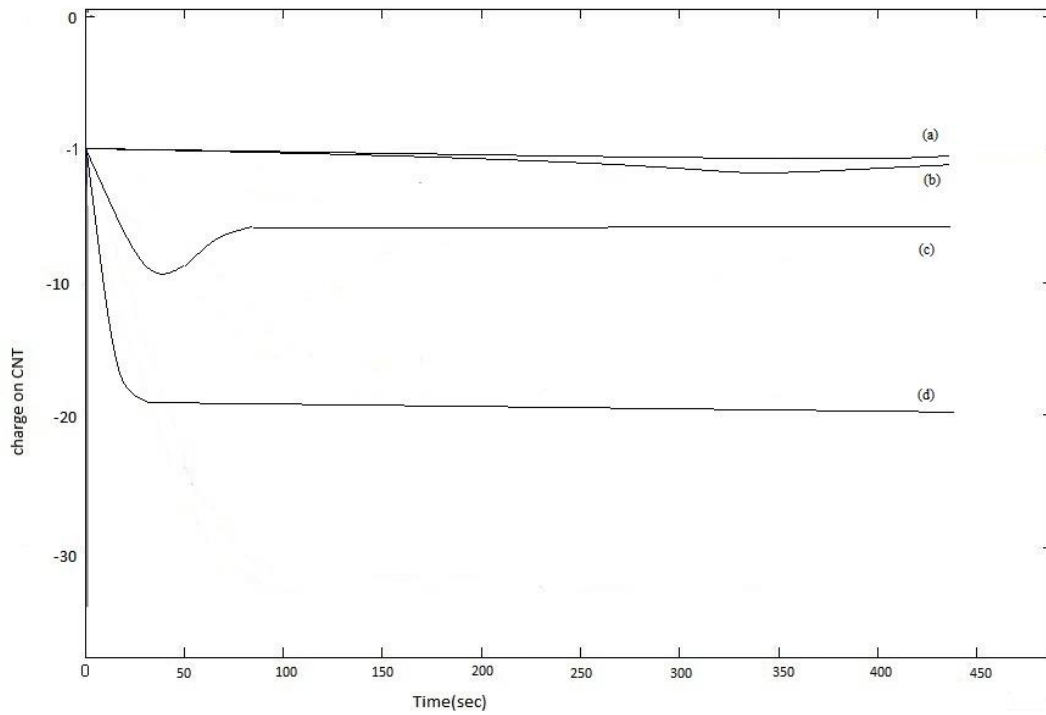


Fig.1. It shows variation of charge w.r.t time on the surface of CNT

The above Fig. 1 shows the variation of charge on the CNT surface with increase in the substrate potential. From this result we would know that as the substrate potential is increases At (a) $U_s = -30 V$, (b) $U_s = -60 V$, (c) $U_s = -120V$, (d) $U_s = -180 V$, the surface of the CNT is more negatively charged.

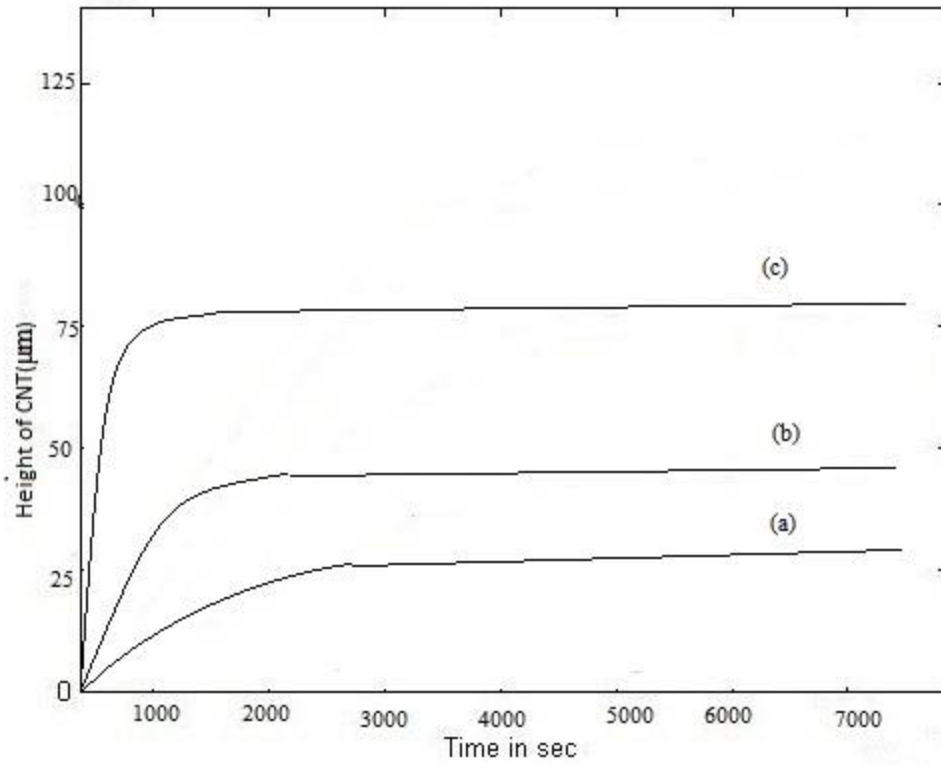


Fig. 2. It shows the variation of height of CNT for different ion density of and temperature of type A. From the above fig. 2. We would know about the variation of height of CNT with the change in temperature and ion no density At (a) $n_{iA0} = 1.2 \times 10^9 \text{ cm}^{-3}, T_{i0} = 1800 \text{ K}$ (b) $n_{iA0} = 4.8 \times 10^9, T_{i0} = 2000 \text{ K}$ (c) $n_{iA0} = 5.6 \times 10^9, T_{i0} = 2200 \text{ K}$. As the temperature and ion number density increases the height of CNT is also increases.

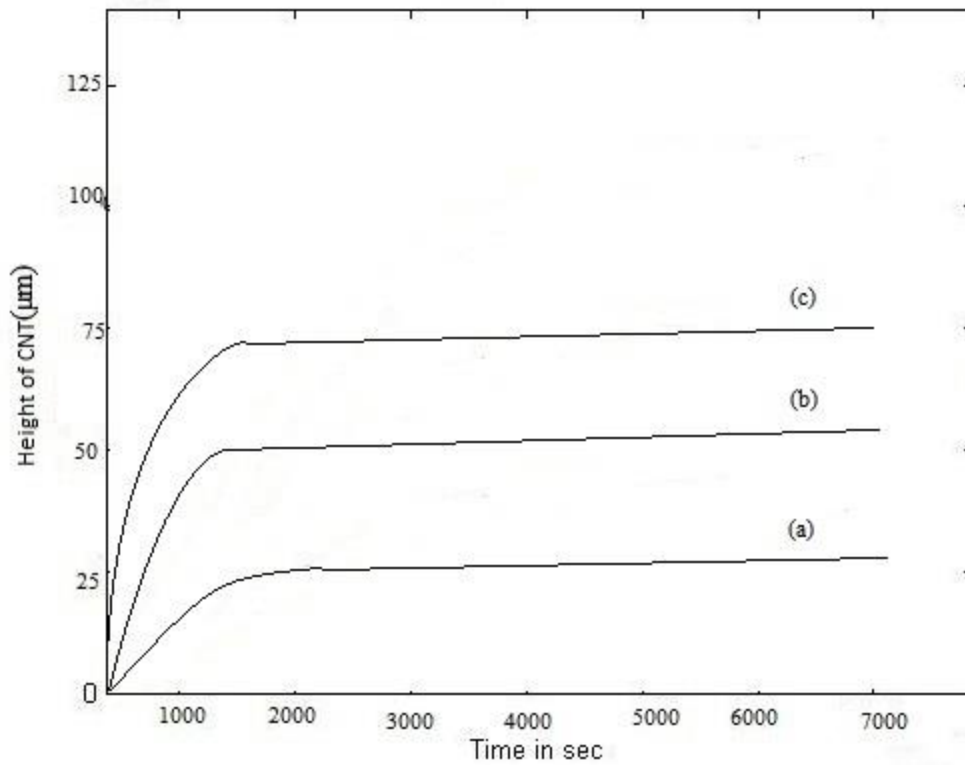


Fig. 3. It shows the variation of height of CNT with different substrate temperature.

When we increase the negative substrate potential on the surface of CNT negative more charge is developed on surface.

At, (a) $T_s = 1600 K$, (b) $T_s = 1900 K$, (c) $T_s = 2200 K$

Due to increase in substrate temperature rate of dissociation of methyl ion increased and more deposition of carbon is takes place at the surface of CNT. It leads to increase in the height of CNT with change in substrate potential.

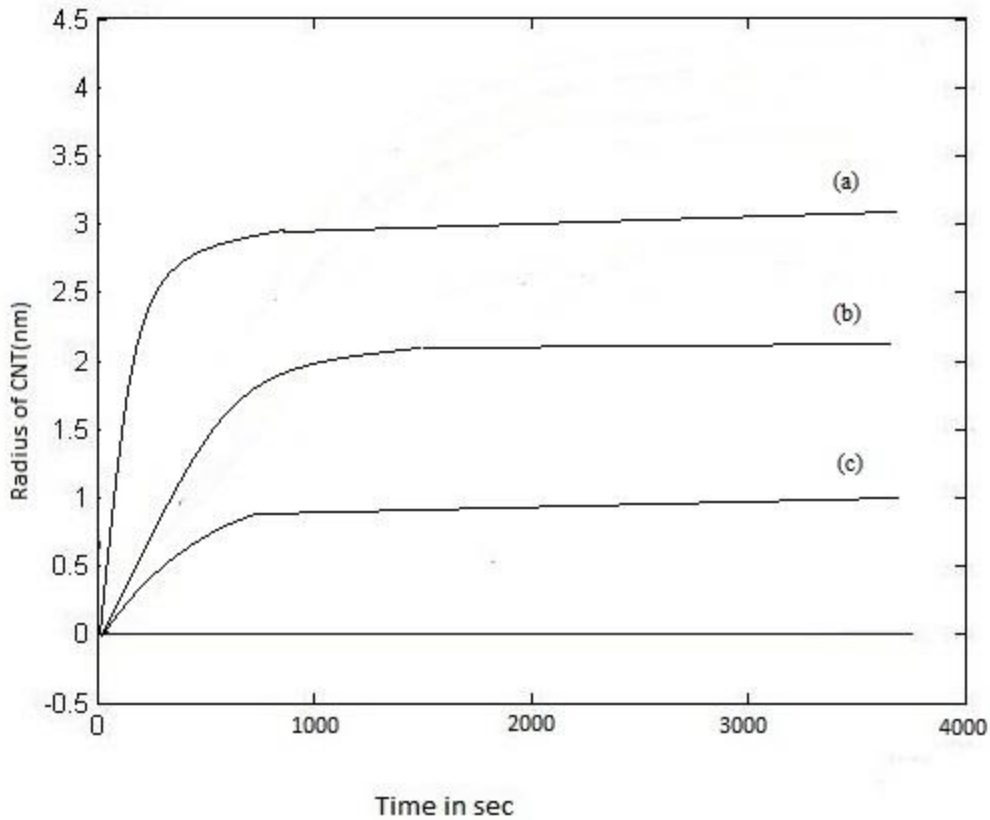


Fig. 4. It shows the variation of Radius of CNT tip for different ion density and temperature of type B.

When the ion number density and temperature is changed then the variation in the radius of CNT is taking place. At (a) $n_{iB0} = 1.2 \times 10^9$, $T_{i0} = 1800 K$, (b) $n_{iB0} = 5.6 \times 10^{10}$, $T_{i0} = 2000 K$, (c) $n_{iB0} = 1.3 \times 10^{11}$, $T_{i0} = 2200 K$.

It is attributable to the fact that the CNT tip is bombarded by hydrogen ions, which engraves the CNT tip. At high temperature and density methane gas easily dissociate into carbon and hydrogen ions, where carbon is responsible for the length of CNT while hydrogen shapes the nanoparticle tip radius.

From the above fig. 4 we got to know that as the ion number density and temperature increases the radius of the CNT hemispherical tip is decreases.

CHAPTER 5

Conclusion

In this theoretical model, we are taking care of charging rate on the surface of the cylindrical CNT with Hemispherical Tip. Kinetic equation of neutral atoms, ions and electron, growth rate equation of the curved surface of CNT is also in the consideration due to diffusion and gradual accumulation of additional layers of ions on catalyst nanoparticle addition is subjected to plasma sheath is developed.

We are taking the radius of Ni catalyst fixed, which serve as the initial condition for the growth of the nanotube. We came to know about the effect of ion density and temperature on the radius and height of the CNT. The substrate bias effect on the charge of CNT and height of CNT is also studied and result shows sufficient accuracy.

This work is useful for the manufacturing of the high aspect ratio carbon nanotube desirable for the field emission device.

References

1. Anthuvan Rajesh John, Pandurangan Arumugam. Studies on structural and magnetic properties of pristine and nickel-filled carbon nanotubes synthesized using LaNi₅ alloy particles as a catalyst. *Chemical Engineering Journal* 243 (2014) 436–447.
2. Uhland Weissker , Silke Hampel, Albrecht Leonhardt, Bernd Buchner. Carbon Nanotubes Filled with Ferromagnetic Materials. *Materials* 2010, 3, 4387-4427.
3. D. Ostling, D. Tomanek, A. Rosen. Electronic structure of single-wall, multiwall, and filled carbon nanotubes. 1997 The American Physical Society, 0163-1829/97/55(20)/13980~9.
4. M. Monthieux. Filling single-wall carbon nanotubes. *Carbon* 40 (2002) 1809 –1823.
5. Victor M. Garcia-Suarez , Jaime Ferrer , Colin J. Lambert. Tuning the electrical conductivity of nanotube-encapsulated metallocene wires.
6. H. Kataura, Y. Kumazawa , Y. Maniwa , I. Umezu , S. Suzuki , Y. Ohtsuka, Y. Achiba. Optical Properties of Single Wall Carbon Nanotubes. *Synthetic Metals* 103 (1999) 2555-2558.
7. Jianchun Bao,Quanfa Zhou, Jianming Hong,Zheng Xu.Synthesis and magnetic behavior of an array of nickel- filled carbon nanotubes. *Appl. Phys. Lett.*, Vol. 81, No. 24, 9 December 2002.
8. R. J. a. C. R. Bertozzi, "Progress and challenges for the bottom-up synthesis of carbon Nanotubes with discrete chirality," *Chemical Physics Letters*, vol. 494, pp. 1-7, 2010.
9. M. P. a. T. Goswami, "Carbon nanotubes – Production and industrial applications," *Materials & Design*, vol. 28, pp. 1477-1489, 2007.
10. C. S. , M. C. a. W. I. M. Kenneth B.K. Teo, "Catalytic Synthesis of Carbon Nanotubes and Nanofibers," American Scientific Publishers, 2003.
11. H. D. J. L. K. H. a. A. H. W. Ernesto Joselevich, "Carbon Nanotube Synthesis and Organization," *Applied Physics*, vol. 111, 2008.
12. C. H. Z. J. J. L. a. Y. L. Naiqin Zhao, "Fabrication and growth mechanism of carbon Nanotubes by catalytic chemical vapor deposition," *Material Letters*, vol. 60, pp. 159-163, 2006.
13. H. D. J. L. K. H. a. A. H. W. Ernesto Joselevich, "Carbon Nanotube Synthesis and Organization," *Applied Physics*, vol. 111, 2008.
14. C. Binns, *Introduction to Nanoscience and Nanotechnology*, New Jersey: John Wiley & Sons, pp. 121-127,2010.

15. J. D. C. H. J. A. a. R. K. Jan Prasek, "Methods for carbon nanotubes synthesis—review," *Journal of Materials Chemistry*, vol. 21, p. 15872–15884, 2011.
16. V. M. T. M. M. G. a. K. K. A.V. Melechko, "Vertically aligned carbon nanofibers and related structures: Controlled synthesis and directed assembly," *Journal of Applied Physics*, vol. 97, 2005.
17. Y. Z. R. L. a. X. S. Mihnea Ioan Ionescu, "Selective growth, characterization, and field emission performance of single-walled and few-walled carbon nanotubes by plasma enhanced chemical vapor deposition," *Applied Surface Science*, vol. 258, pp. 1366-1372, 2011.
18. T. N. a. K. Okazaki, "Carbon nanotube synthesis in atmospheric pressure glow discharge: A review," *Plasma Processes and Polymers*, vol. 5, pp. 300-321, 2008.
19. M. J. Goeckner, "Aspect of Plasma Processing: A brief overview of plasma science in industry," UTD, [Online]. Available: http://www.utdallas.edu/~goeckner/plasma_sci_class/Plasma%20Process%203%20Types.pdf. [Accessed 30 04 2012].
20. R. L. Spencer, "A brief Introduction to Plasma Physics," [Online]. Available: <http://maxwell.byu.edu/~spencerr/phys442/plasma.pdf>.
21. M. J. Goeckner, "Aspect of Plasma Processing: A brief overview of plasma science in industry," http://www.utdallas.edu/~goeckner/plasma_sci_class/Plasma%20Process%203%20Types.pdf. [Accessed 30 04 2012].
22. S.-Y. K. a. H.-W. L. Sang-Gook Kim, "Effect of ammonia gas etching on growth of vertically carbon nanotubes/nanofibers," *Transactions of Nonferrous Metals Society of China*, vol. 21, pp. 130-134, 2011.
23. Y. Z. R. L. a. X. S. Mihnea Ioan Ionescu, "Selective growth, characterization, and field emission performance of single-walled and few-walled carbon nanotubes by plasma enhanced chemical vapor deposition," *Applied Surface Science*, vol. 258, pp. 1366-1372, 2011.
24. T. N. a. K. Okazaki, "Carbon Nanotubes synthesis in atmospheric pressure glow discharge: A review," *Plasma Processes and Polymers*, vol. 5, pp. 300-321, 2008.
25. h. W. a. J. J. Moore, "Different growth mechanisms of vertical carbon Nanotubes by rf- or dc plasma enhanced chemical vapor deposition at low temperature," *American Vacuum Society*, 2010.
26. C. D. a. J. R. S. Hofmann, "Low-temperature growth of carbon nanotubes by plasma enhanced chemical vapor deposition," *Applied Physics Letters*, vol. 83, no. 1, 2003.

- 27.** E. B. a. E. J. Burak Caglar, "Production of carbon nanotubes by PECVD and their applications to supercapacitors".
- 28.** R. C. L. D. Y. L. W. Z. Y. Z. Z. J. F. P. a. J. L. Yan Li, "How Catalysts Affect the Growth of Single-Walled Carbon Nanotubes on Substrates," *Advanced Materials*, vol. 22, pp. 1508-1515, 2010.
- 29.** A. Tewari, S. C. Sharma, *Physics of Plasmas; Modeling carbon nanotube growth on the catalyst-substrate surface subjected to reactive plasma*, 063512 (2014); doi: 10.1063/1.4885104.
- 30.** M. A. Lieberman and A. J. Lichtenberg, *Principles of Plasma Discharges and Materials Processing* (Wiley Interscience Publication, USA, 1994).
- 31.** A. Tewari, S. C. Sharma, *Physics of Plasmas; Modeling carbon nanotube growth on the catalyst-substrate surface subjected to reactive plasma*, 063512 (2014); doi: 10.1063/1.4885104.
- 32.** A. Tewari, S. C. Sharma, *Physics of Plasmas; Modeling carbon nanotube growth on the catalyst-substrate surface subjected to reactive plasma*, 063512 (2014); doi: 10.1063/1.4885104.
- 33.** S. C. Sharma, A. Tewari, *Can. J. Phys.* 89, 875 (2011).
- 34.** P. K. Dubey, *J. Phys. D: J. Appl. Phys.* 3, 145 (1970).
- 35.** A. Tewari, S. C. Sharma, *Physics of Plasmas; Modeling carbon nanotube growth on the catalyst-substrate surface subjected to reactive plasma*, 063512 (2014); doi: 10.1063/1.4885104.
- 36.** A. Tewari, S. C. Sharma, *Physics of Plasmas; Modeling carbon nanotube growth on the catalyst-substrate surface subjected to reactive plasma*, 063512 (2014); doi: 10.1063/1.4885104.